特輯

Vibration Problems in Mechatronics

S. CHONAN and Z.W. JIANG
Department of Aeronautics and Space
Engineering, Tohoku University, Sendai, Japan.

Ⅰ. Introduction

Advances in technology have accelerated the development of machines and instruments that make the features of high-speed operation and less energy consumption. To meet such requirements their constituents should be designed simple and light, which necessarily means that the total system rigidity is decreased and the constituents are easily excited by the internal as well as the external disturbances.

This note is an introduction to the vibration phenomena that are commonly observed on the modern electro-mechanical machinery, together with the recommended countermeasures to control the system vibrations.

Ⅱ. Axially Moving Blades

The problem of axially moving materials is a subject of technological interest since many such materials are observed in manufacturing industries.[1-10]

Some decades ago, the typical examples were rolled threadlines and steelbelts, and bandsaw blades cutting the lumber. Nowadays they are observed in the form of magnetic tapes in the information storage system, and multi-band saws and wire saws slicing the silicon ingot. These axially running materials are modeled in general as shown in Figure 1.

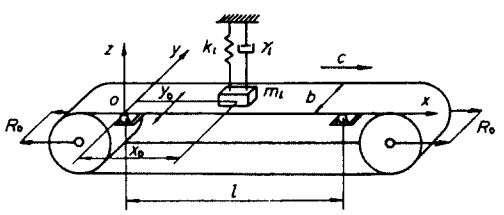

Fig. 1. Axially moving strip with mass-spring-dashpot system.

The thin blade is moving with a constant speed c in the positive axial direction. Further, a space-fixed mass-spring-dashpot system is being attached to the blade at the point(x_0, y_0). The attached aditional system is, for sample, the magnetic head reading or writing data from the running tape. To study the dynamics of the system, it is necessary first to formulate the problem. Commonly, the analysis is started from the construction of the governing equations. The equation of the motion of the blade described with respect to the co-ordinate frame fixed in space is.[11]

$$D\nabla^4 w+\gamma(c\partial/\partial x+\partial/\partial t)w-N_x\partial^2 w/\partial x^2$$
$$=-[(m_t\partial^2/\partial t^2+\gamma_t\partial/\partial t+k_t)w]\delta(x-x_0)\delta(y-y_0) \quad (1)$$

where

$$\nabla^4=(\partial^2/\partial x^2+\partial^2/\partial y^2)^2,$$
$$D=Eh^3/12(1-\nu^2),$$
$$N_x=R_0/b+(1-x)\rho hc^2.$$

Here, w is the lateral displacement of blade, D is the flexural rigidity, E is the Young's modulus, ρ is the mass density, υ is the Posson's ratio, and γ is the external coefficient of damping; h and b are the thickness and width of blade, N_x is the in-plane axial tension, R_0 is the initial tension, and c is the running speed of blade; x($0 \le x \le 1$) is the stiffness of wheel support.[11] Further, k_t, m_t, and γ_t are the stiffness, mass and damping coefficient of the space-fixed attached system.

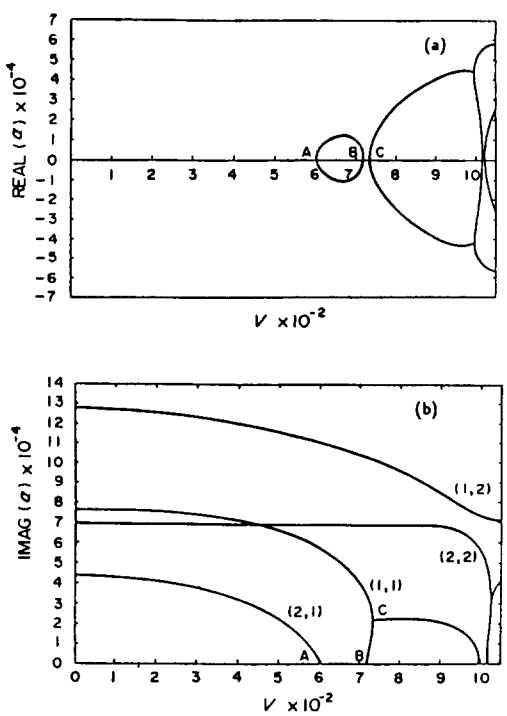

Fig. 2. Complex frequency-speeddiagram. x=1, $\alpha=p\,[ph^5/D]^{1/2}$, $\upsilon=c/[D/ph^3]^{1/2}$, ℓ/b=10.0, ℓ/b=500, (x_0/ℓ, y_0/b)=(0.5, 1.0), m_t/ph^3 =1.6667×10³, $k_t h^2/D$ =0.08, $\gamma_t/[ph\ D]^{1/2}$= 0.0, $\gamma/[D\rho/h^3]^{1/2}$=0.0, R_0h/D=0.17333.

For the case of magnetic tapes and wire saws, the flexural rigidity D is small compared with their other physical parameters, and it is generally assumed zero in the theoretical analysis. Further, for the case of the wire, the width b is small and $\partial w/\partial y = 0$ is common-ly assumed in the analysis. The solution of equation (1) is generally assumed in the form

$$w(x,y,z)=\sum_{m=1}^{\infty}\sum_{n=1}^{\infty}X_m(\cdot)Y_n(y)A_{mn}(t), \quad (2)$$

where X_m and Y_m are the mode functions satisfying the boundary conditions of the blade. Substituting Eq.(2) into Eq.(1) and applying the Galerkin method to the resulting equations, one has a system of simultaneous differnetial equations in A_{mn}(t), which are solvedby applying the conventional methods of analysis on the free and forced vibrations of the system.

Figures 2 (a) and (b)[11] show the variations of the real and imaginery parts of the frequency parameter α versus the nondimensional axial speed of blade ν. IMAG(α) is the natural frequency while REAL(α) is the damping coefficient when the time function is given in the form

$$A_{mn}(t)=\bar{A}_{mn}\exp(\alpha T), \quad (3)$$

where

$$\alpha=p[ph^5/D]^{1/2}, T=t[ph^5/D]^{-1/2}$$

The figure shows that the moving blade has many natural frequencies and they are increased or decreased depending on the moving speed of blade. The symbol (m,n), m,n = 1,2,⋯, attached to the curve means that the frequency is the one for the mode with the m-and n-th vibration modes in the x-and y-directions, respectively. In the figure, $\upsilon=1\times10^{-2}$ corresponds to the actural moving speed of c =15.7m/s for the

steel blade. The(2,1) curve decrease monotonically with an increase of the speed and becomes zero at $\nu = 6\times10^{-2}$.

It is well known that the system resonance frequency corresponds to the natural frequency. Thus, the zero natural frequency means that the system encounters a resonance(static resonance) when it is subjected to a static load such as the reaction force from the cutting lumber or the magnetic read/write head. The moving speed of blade for which the static resonance appears is generally referred to as the critical speed.

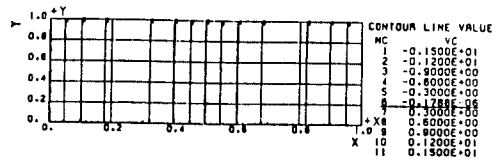

(a) Mode (2,1)

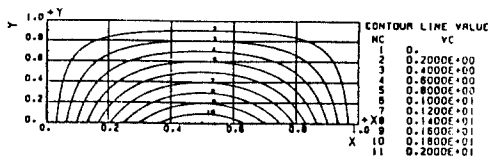

(b) Mode (1,1)

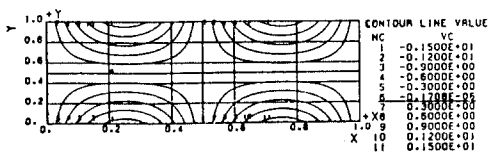

(c) Mode (2,2)

Fig. 3. Mode shapes of blade at the (a) first, (b)second and (c)third critical speeds of Fig. 2. The physical parameters are same as Fig. 2.

When the moving speed is greatert han the critical speed, the frequency has a positive real part and the amplitude of blade becomes greater with time, which means that the first critical speed is actually the maximum operation speed for the axial moving materials. The existence of the critical speed is a feature characterizing the dynamics of axially moving elastic materials. Figure 3 shows the mode shapes of the blade at the critical speeds A, B and C given in Fig. 2(a).

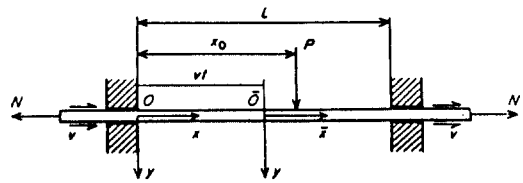

Fig. 4. Axially moving saw subjected to space-fixed reaction from workpiece.

The band saw or wire saw slicing a silicon ingot is subjected to a static reaction force from the ingot. Figure 4[12] shows the axially running saw blade subjected to a constant lateral force P which is resting statically in space. Figures 5 and 6[12] are the variations of the blade deflection with an increase of the axial speed v. In the figure, E is the Young's modulus, A the cross-sectional area, and N the initial axial tension; ρ is the mass density, ℓ the length and h the thickness of blade, respectively. v is the non-dimensional running speed of blade and v=0.1 corresponds to the actual speed of v=50m/s for the steel sawblade.

The static lateral load is located at $x_0'(=x_0/\ell)$=0.4 and shown with an arrow in the figure. The blade is translating in the positive $x'(=x_0/\ell)$ direction with a constant speed, while the deformation pattern is time invariant when observed from the space-fixed co-ordinate frame. Every parts of the blade follow the same path when they translate from left to right. It is seen that the deforma-

tion pattern and the response amplitude vary considerably with an increase of the axial tension and the running speed of blade.

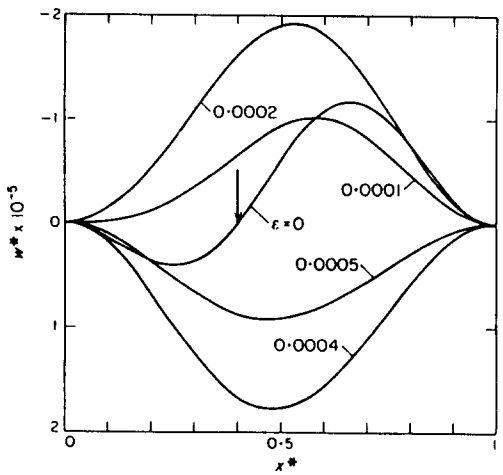

Fig. 5. Variation of displacement profile of axially moving saw blade with increasing axial tension $\epsilon(=[EA]^{-1}N)$.→, Position of applied load: $w^{*}=[EA/ph]w$, $[E/\rho]^{1/2}=0.025$, $\ell/h=100$, $x_0/\ell=0.4$.

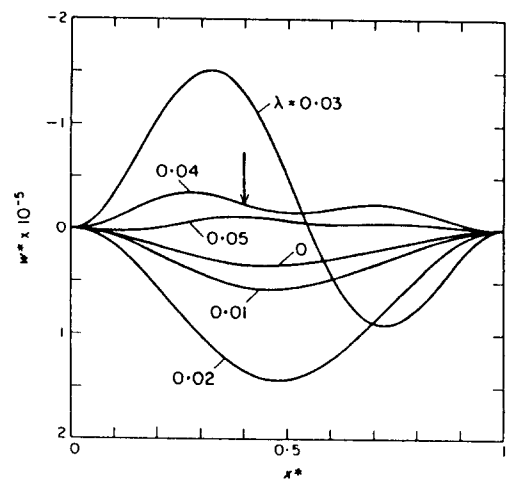

Fig. 6. Variation of displacement probile of axially moving saw blade with increasing axial speed $\lambda(=[E/\rho]^{1/2}\nu)$.→, Position of applied load: $w^{*}=[EA/ph]W$, $\ell/h=100$, $[EA]^{-1}N=0.0002$, $x_0/\ell=0.4$.

Ⅲ. Rotating Circular Blades

The rotating circular blade is commonly observed in manufacturing industies. It is the fundamental element of machines such as the steam and gas turbines, grinding wheels, circular saws, and computer head disk assemblies. Large amplitude transverse vibration of the rotating blades can be a cause of the fatigue failure of turbine wheels, the cutting inaccuracy of grinding wheels and circular saws, and the head tracking error to computer disk memory. It is therefore of technological importance to investigate the dynamics of circular plates and improve their durability and robustness to the dynamic loading.[13][25]

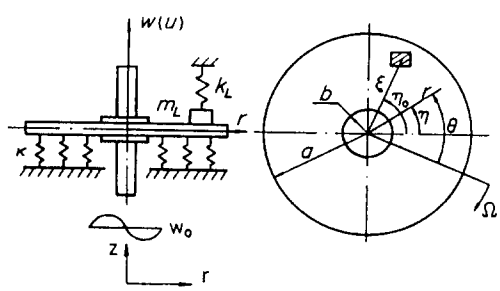

Fig. 7. Head-disk assembly.

Figure 7[26] shows a disk of outer radius *a* and inner radius *b* rotating at a constant angular speed Ω in the clockwise direction. In some cases, the disk system is excited by an external axial or pitching displacement w_0, or it is subjected to an external cutting force for the case of the saw blade, or the reaction from the read/write head in the case of the computer disk. For the spinning disk excited in the transverse direction, three coordinate frames are introduced in the theoretical analysis. They are the frame rotating with the disk but stationary in transverse

direction (z, r, θ), the frame rotating with the disk and fixed on to the rotating disk (w, r, θ) and the frame fixed on to the rotating disk but not rotating with the disk (u, r, η). The radial coordinate r is common in three cases, while the other coordinates are related each other through $z=w+w_0$, $u=w$ and $\theta=\eta+\Omega t$, where w_0 is the external displacement to the disk.

The equation of motion for a freely rotating disk is written in the form

$$D\nabla^4 w + ph\partial^2 w/\partial t^2 - (h/r)(\partial/\partial r)(\sigma_r r\partial w/\partial r) - (h/r)(\partial/\partial\theta) = 0, \quad (4)$$

where

$$\nabla^4 = [\partial^2/\partial r^2 + \partial/r\partial r + \partial^2/r^2\partial\theta^2]^2,$$
$$D = Eh^3/12(1-\nu^2).$$

Here w is the deflection, D the flexural rigidity, E the Young's modulus, ρ the density and ν Poisson's ratio. Further σ_r and σ_θ are the centrifugal stresses due to the disk rotation.

To solve Eq.(4), the coordinate is first transformed to the space-fixed stationary coordinate (u, r, η) and then the solution is assumed in the form

$$u(r,\eta,t) = \sum_{m=0}^{M}\sum_{n=0}^{N}[C_{mn}(t)\cos(n\eta) + S_{mn}(t)\sin(n\eta)]R_{mn}(r), \quad (5)$$

where R_{mn} are the mode functions of a non-rotating disk satisfying the boundary conditions. The rotating disk problem can be solved by substituting Eq.(5) into Eq.(4) further applying the Galerkin method to the resulted equation.

Figure 8[27] shows the nondimensional natural frequencies Φ_0 of an aluminum blade as functions of the nondimensional revolution speed Ω_0. The dashed lines show the experimental results and the solid lines the theoretical results. The symble (m, n) indicates the vibration modes with m nodal circles and n nodal diameters. For example, (0,3) means that the blade vibrates with 0 nodal circles and 3 nodal diameters on the blade.

For the non-rotating disk ($\Omega_0=0$), just one natural frequency is observed on each vibration mode, while for the rotating disk each mode other than (0,0) mode has two frequencies. This is due to the fact that the disk response is composed of two waves, the progressive and the regressive waves. The progressive wave travels in the same direction as the disk rotation while the regressive wave rotates in the opposite direction to the disk rotation. For the (0,0) mode, the waves have an infinite angular speed thereby no separate waves observed. It may also be seen that the upper frequency becomes greater while the lower frequency decreases monotonically with an increase of the rotation speed of disk. The lower natural frequency decreases to zero at a certain rotation speed generally referred to as the critical speed, where the static divergence instability appears on the blade. All vibration modes except (0,0) and (0,1) have the critical speed.

It depends on the radii ratio of the blade b/a which mode brings the lowest critical speed, where b and a are the inner and outer radii of blade. The (0,2) mode has the lowest critical speed for the disk with $b/a=0 \sim 0.2$, while it is transferred to (0,3) and (0,4) modes as b/a increases.[28]

Figure 9[26] shows the response curve of a rotating floppy disk which is subjected to an axial excitation. Figure 9(a) is the response of a freely rotating disk without a read/write head and Fig.9(b) the case of a disk with the head. Only the vibration mode with 0 nodal diameters appears on the disk(Fig.9a), while all vibration modes are excited when the head or the spring guide is attached to the disk(Fig.9b).

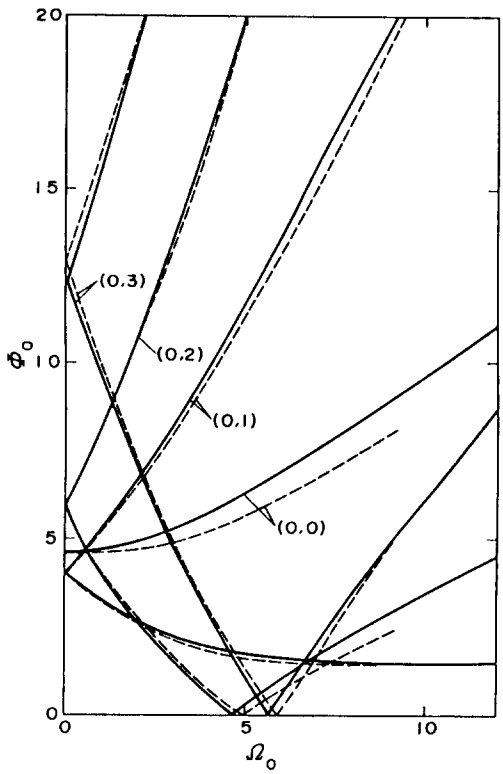

Fig. 8. Natural frequencies Φ_0 as functions of revolution speed Ω_0.

The disk unit is also installed in the portable instrument. For a device such as the video camera, the operation speed is recommended to be 3600 rpm so that it synchronizes with the TV scanning speed. In the 2″ disk system as given in Fig. 10[29], the head is attached to the rotating disk in two ways. In one case, the head presses the disk surface while the stabilizer pushes back the disk from the other side. In the other case, the system has no stabilizer and the head is kept on the disk surface by the negative pressure generated by the disk rotation. It is well known that a flutter type of instability appears on the disk depending on the operation speed and the contact condition of head to disk. The commanded operation speed of 2″ floppy disk is 3600rpm. which is much higher than the 1st critical speed.

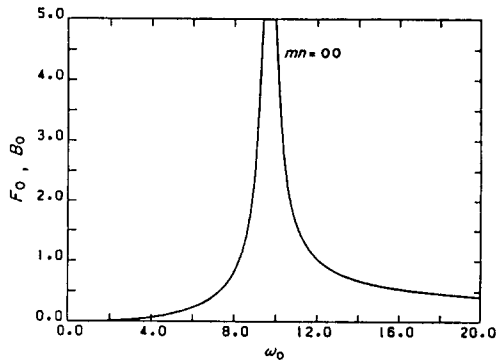

(a) Freely rotating disk

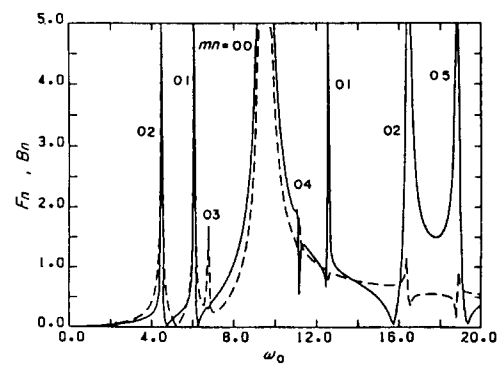

(b) Disk with R/W head

Fig. 9. Deflection response of disk subjected to axial excitation.

Figure 11[29] shows the real part of disk complex frequency σ versus the rotation speed Ω. When the complex frequency has a real part, a flutter-type instability appears on the disk. Figure 11(a) is the case when the disk is equipped with the head. No stable operation speed is obtained when the rotation speed Ω exceeds the the critical speed A(2240 rpm). Figure 11(b) shows the case when an optimum designed stabilizer was attached to

the disk from the opposite side of the head. It is found that the unstable region was much reduced and a stable region was formed around the speed 3600 rpm. In general, the optimum design of the stabilizer is an important problem for the rotating flexible disk.

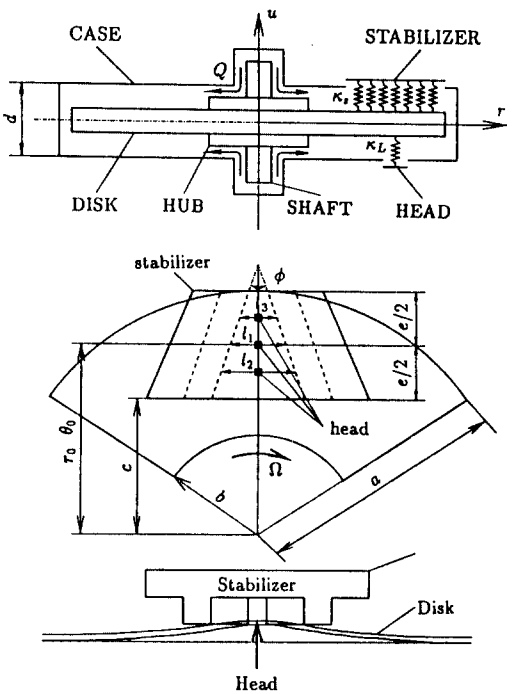

Fig. 10. 2″ disk drive unit.

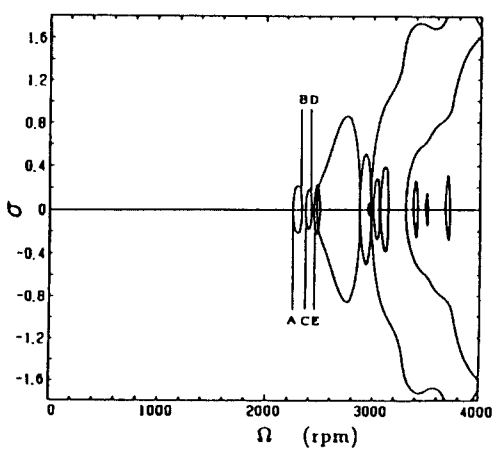

(a) Disk with a head

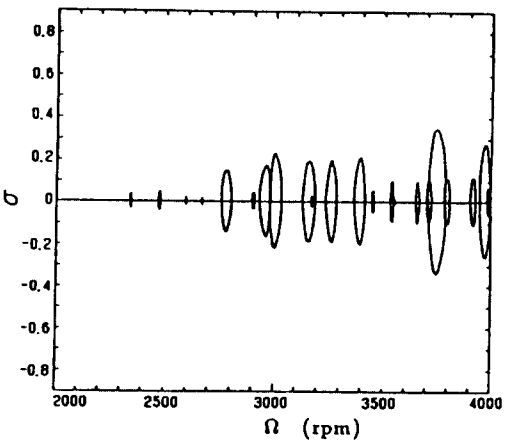

(b) Disk with an optimally designed stabilizer

Fig. 11. Real part σ of complex frequencies versus rotation speed Ω.

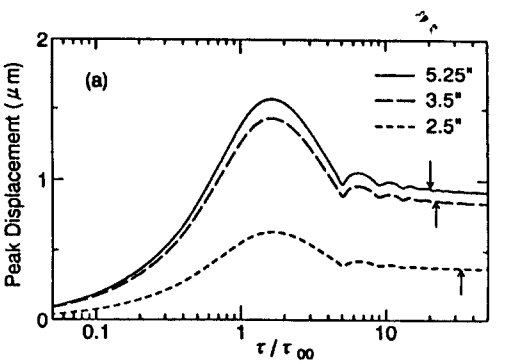

Fig. 12. Variation of peak displacement of disk versus duration of axial excitation.

With the development of information-intensive culture, it has become commonly observed that the electronic equipments are subjected to mechanical disturbances. A typical example is a notebook computer, which is easily get slammed, jolted and bumped while being carried.

The manufacturers give a shock test to the disk drive units commonly by using a half-sine shock pulse with a duration of 11ms.

However, no clear explanation has been given about the scientific basis on adopting the duration 11ms. Nowadays various kinds of disk drives are being developed, which means that a unified approach of using a duration 11ms is no longer applicable in order to evaluate the durability of systems with different structural stiffnesses. Some simulation results have been obtained for the investigation of this problem. Figure 12[30] is the variation of peak displacement of rotating disk as a function of the axial input duration τ.

It is shown that the peak displacement that appears on the disk takes on the maximum when the input duration τ is about 1.5 times the half period τ_{00} of the fundamental (0,0) mode. Further, the shock pulse with a duration 11ms, which is nowadays a standard input to the shock test of disk drive units, brings only 60-70% of the maximum displacement that may appear on the rotating disk.

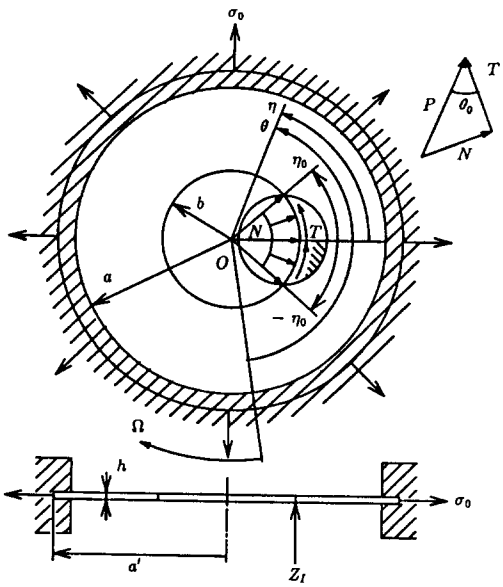

Fig. 13. Silicon wafer slicer cutting crystal ingot.

Another high-tech application of the circular blade is the production of silicon wafers in the semiconductor industry.

The ID(inner-diameter) saw blade shown in Fig.13[31] is commonly used in the crystal wafering. One example of the blade is a 0.15mm thin annular SUS304 blade with diamond abrasive at the inner edge (0.24m in diameter) while clamped from both sides along the outer periphery (0.625m in diameter). The blade is tensioned initially at the outer edge, while the inner periphery is acted upon by the in-plane radial compressive force N and the circumferential shear force T.

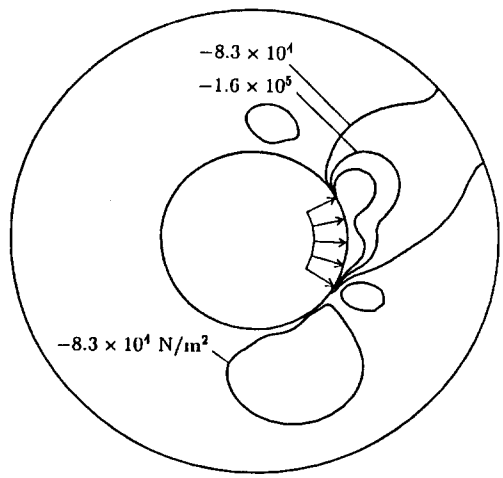

Fig. 14. Contour-line map of shear stress induced by slicing load.

Figure 14 [32] shows the distributions of shear stress in the blade due to the slicing load represented on the contour-line map. It is observed that the stresses are distributed in the blade asymmetrically and are maximum at the inner periphery. Demands on large-diameter silicon wafer(6—12 inch) have accelerated the development of the large-scale slicer. Further, high performance of the IC devices has made it a necessity to

provide wafers with adequately flat, parallel sides. It seems that the introduction of active control is indispensable to meet these requirements and develope a highly efficient slicer.

Ⅲ. Flexible Robot Arms

The needs for more precise positional accuracy, higher load capacity, lighter members and higher operation speeds have made it a necessity to take into account the flexibility of links in the control of industrial robotic manipulators, and many papers have been published on this matter during the past years.[34][39] Figure 15 shows a one-link flexible robot arm having an end effector at the tip and driven by a motor at the shoulder.

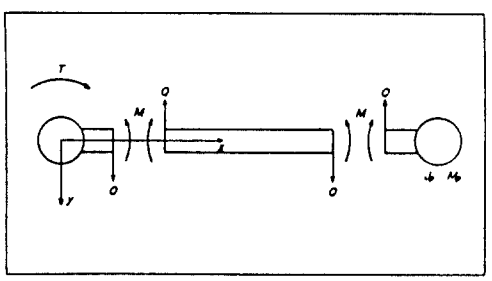

Fig. 15. Flexible robotic arm driven by shoulder motor.

The optimum design of the system and the controller can be done effectively with the aid of the computer simulation. Generally, the theoretical analysis of the flexible arm is started from the equation of motion given by

$$\bar{E}I\partial^4 w/\partial x^4 + pA\partial^2 w/\partial t^2 = 0, \quad (6)$$

where

$$\bar{E} = E(1 + c\partial/\partial t).$$

Here, w is the lateral displacement, E the Young's modulus, ρ the mass density, I the moment of inertia, A the cross-sectional area, c the internal damping coefficient of beam, and t the time. To solve Eq. (6), it is necessary to formulate the boundary conditions.

They are obtained by considering the equilibria of moments and forces that are acting on the shoulder and the armtip. The governing equations can be solved, for example, by applying the modal expansion method or the Laplace transform method with respect to both the space variable and the time.

One of the effective algorithms to achieve high speed control of flexible manipulators is the simple scheme of tip sensing and base torquing. Figure 16(a) and (b) show the displacement of a lightweight robotic arm driven by this scheme.

Figure 16(a) is the displacement when the shoulder motor was rotated stepwise by the amount of $\dot{w}_d/L$, where $\dot{w}_d$ is the desired tip displacement and L is the length of arm.

This is a classical open-loop control having been applied commonly to the control of rigid arms. As can be seen, the time decrement of curve is rather slow and the arm tip continues to fluctuate around its commanded position.

Figure 16(b) shows the tip displace-ment when the arm is driven by the PD con-trol scheme using the sensor's measurement of actual tip position as a feedback signal. It is clear that the scheme of tip sensing and base torquing is quite effective to achieve a high-speed point-to-point (PTP) control of the arm.

One typical example of the flexible arm is the module on-board multi-link space manipulator. Figure 17[40] shows a two-link flexible arm with two shoulder and elbow joint motors. Figure 18[40] shows the first four

natural frequencies of the two-link system plotted as functions of the elbow angle.

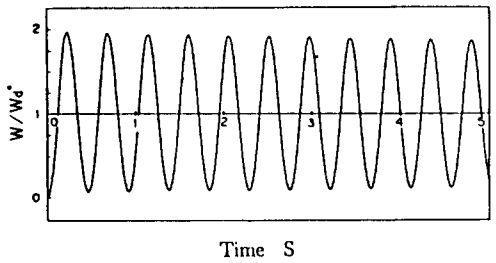

(a) Step rotation at shoulder:

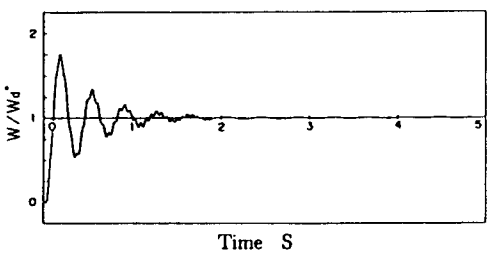

(b) Feedback control by tip sensing and base torquing.

Fig. 16. Tip displacement of flexible robot arm to step input(experimental results).

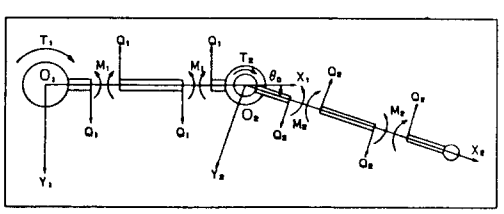

Fig. 17. Two-link flexible arm

Here, the elbow angle is the rotational angle of the second arm relative to the first arm. Curves I and III show the first and the second natural frequencies of the in-plane vibration of links, and curves II and IV the frequencies for the out-of-plane vibration of the system.

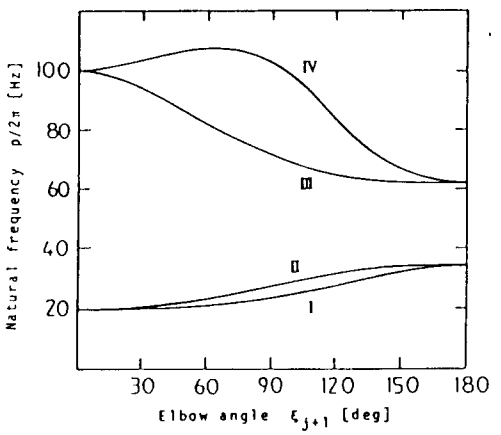

Fig. 18. First four natural frequencies of two-link flexible armversus elbow angle. Curves I and III, in-plane vibration: curves II and IV, out-of-plane vibration.

It is seen that the frequencies are varied dependent on the eblow angle, which means that the stiffness of the system is changed and the control gains should be adjusted appropriately based on the system configuration.

Figure 19 [41] shows the results of the PTP control to the step command elbow and tip locations $\{y_{d1}\ y_{d2}\}=\{y_{d1}\ y_{d2}\}$ $H(t)=\{2.5\text{mm}, 5.0\text{mm}\}$ $H(t)$.

The two links are slender aluminum beams of length 20 cm (upper arm)and 50 cm (lower arm). In the figure, Y_1 and Y_2 are the nondimensional tip displacement of links defined by $Y_j=y_j(L_j, t)/y_{dj}$, $j=1, 2$. θ_1 and θ_2 are the rotation angles of the shoulder and elbow joint motors.

The controller is the decentralized PD controller. The two joint motors are driven respectively by using the endpoint informa-

tion from the other side. It is seen that the high speed control without overshoot is realized when the feedback gains were selected appropriately.

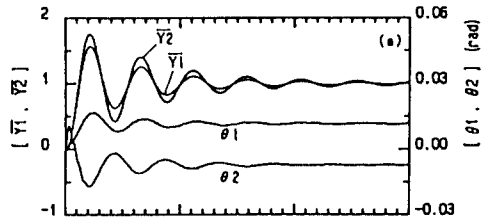

(a) Experimental results for a set of feedback gains:

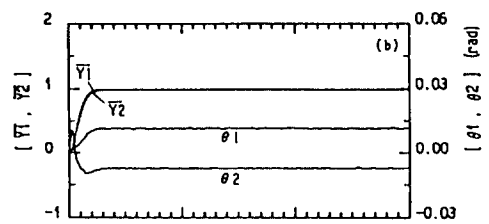

(b) Experimental results for optimum set of feedback gains:

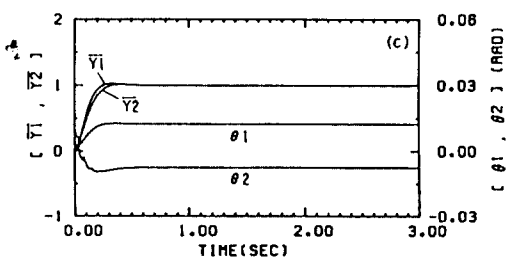

(c) Theoretical results to(b).

Fig. 19. Response of two-link flexible arm to step command elbow and tip locations. Control of shoulder and elbow motorsusing respectively their endpoint informations.

Ⅴ. Micro Robotic Gripper

With the development of robotic manipulators, more sophisticated and functional motions are being demanded on the end effector or the finger that handles small objects such as semi-conductor IC chips and microbes. In order to deal with such objects, it is required to assemble a dexterous artificial finger, which necessarily means that highly efficient compact sensors and actuators are to be developed in advance that can realize the minute force control at the fingertip.

Many papers have been published during past years on the robotic hands and fingers. [42][48] It is noted that most of the robotic hands and fingers developed so far have been actuated by servomotors, stepper motors or pneumatic cylinders and they are driven by tendon or ball screw mechanisms for which the effects of backlash and friction losses are sometime not disregarded. As a new actuator, the shape memory alloy(SMA) has been studied and applied to a miniature gripper.[49] The SMA actuator is driven and controlled by heating and the following radiation from the material. Thus, it is said the SMA is rather an actuator to accomplish slow speed tasks. Recently, much interest has been paid on the piezoelectric actuator that responds rapidly to the variation of the applied voltage signal and produces a large force compared with the mass.[50][54]

Figure 20[55] shows a flexible finger with a force sensor at the tip. A pair of piezoelectric unimorph cells are bended to both sides of the finger. An applied voltage signal to the cells causes one cell to expand while the other to contract, which results in a constant continuous bending moment M_p from $x=0$ to a that drives the finger in the xy -plane.

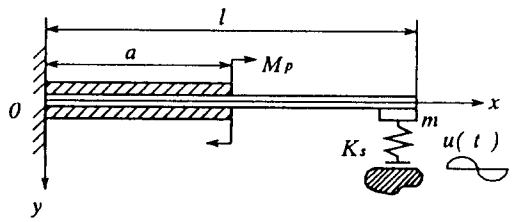

Fig. 20. Robotic finger driven by a pair of piezoceramic unimorph cells.

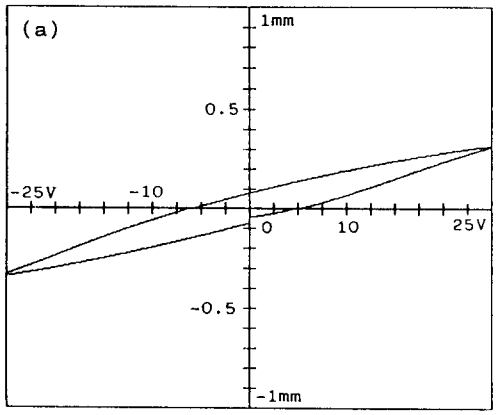

(a)

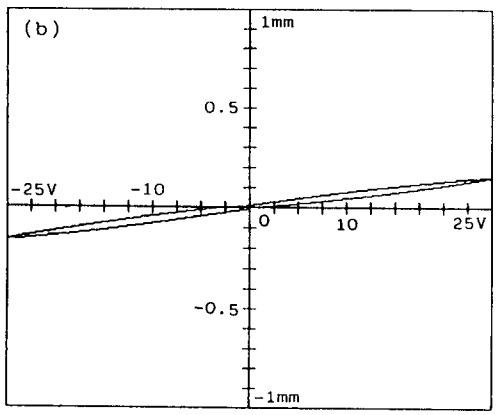

(b)

Fig. 21. Tip hysteresis loop when (a) both cells are driven by the voltage signal ranging from the positive to negtive, and (b) each cell is driven only in the positive/negtive range of voltage.

Piezoelectric ceramics are ferroelectric materials. For this reason they are fundamentally nonlinear in their response to the applied voltage and show a hysteresis loss. Figure 21(a)[56] shows the fingertip displacement when one piezoelectric cell is loaded with the positive voltage and the other cell by the negative voltage and vice versa. It is seen that the displacement curve of the fingertip shows a large hysteresis loop.

It was verified that the hysteresis error can be minimized if one uses each cell only in the positive or negative range of voltage, i.e. when one wish to bend the arm in the positive y -direction, one applies a positive voltage to the lower cell at the same time cuts off the voltage to the upper cell, and vice versa. In this way the hysteresis loop can be reduced over 50 percent in the area as shown in Fig.21(b)[56] and the nonlinear actuator can be modeled as a linear element in the theoretical analysis as well as systematic design of the robotic finger or gripper.

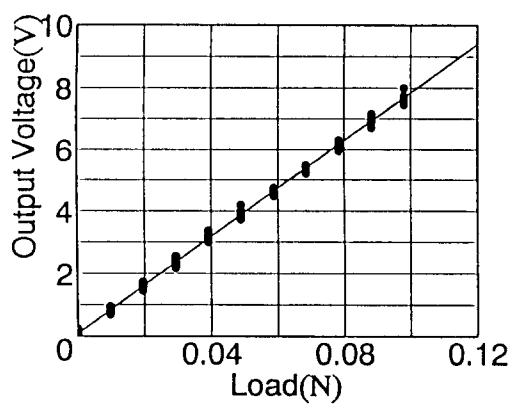

Fig. 22. Output voltage signal from force sensor.

To sense the minute force at the fingertip, it is necessary to introduce a highly efficient force sensor. In our laboratory, a compact

sensor was assembled. It is a square cupper frame of thickness 0.1 mm with a semiconductor strain gauge mounted on the mid span of it, the sensitivity of which is presented in Fig. 22.[55] The output voltage signal from the sensor was measured for five cycles of loading and unloading. It is seen that the sensor output holds the linearity, though some fluctuation is observed. The solid line is the output/input characteristics of the sensor obtained by applying the least square calculation, which shows forces of order 0.01N.

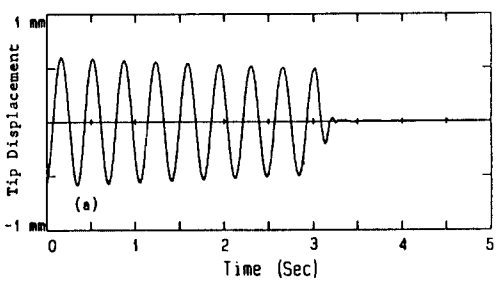

(a)

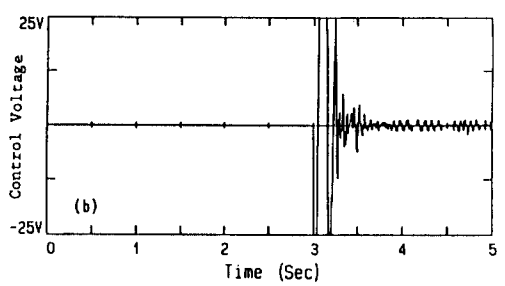

(b)

Fig. 23. Active vibration control of a freely vibrtaing finger: (a) Time variation of tip displacement: (b) Time variation of control voltage to cells.

The following are some experimentally obtained examples showing the efficiency of the piezoelectric cells as actuators in the vibration, position and force control of flexible robotic fingers. Figure 23[56] shows the effectiveness of the piezoelectric actuators in the active control of the vibration. The finger which is vibrating freely is put under the PID control from t=3 sec.

It is seen that the vibration of the fingertip is suppressed and the tip is settled down onto the initial position shortly after the feedback control was started. Figure 23(b) shows the time variation of the input voltage to the cells during the control. It is observed that the cells are working busy to hold the arm tip at the commanded initial position. In the experiment, the maximum voltage applied to the cell was limited to ±25V. It was set automatically to ±25V when the feedback voltage signal exceeds the limits. When the control system was started, the cells are driven by the truncated signal as given in the figure, still it is found that the cells work perfectly to suppress the vibration.

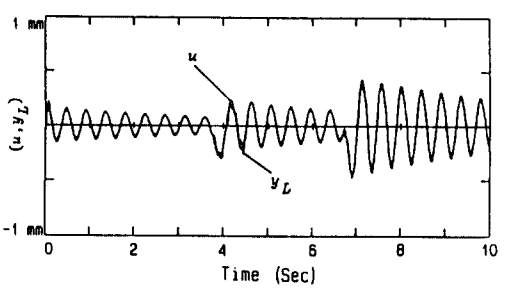

Fig. 24. Displacement of finger tip (y_L) tracking a freely vibrating target surface(u).

Figure 24[56] shows the time response of the fingertip following the surface of freely vibrating cantilever beam which is disturbed three times from the outside. It is clear that the fingertip tracks the target fluctuation tightly when the feedback controller is

designed appropriately.

Figures 25 and 26[57] show the results of the force control of the finger doing two types of holding tasks that are typical to the human forefinger.

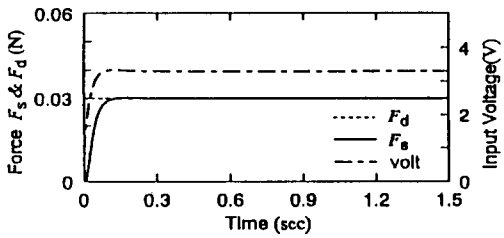

(a) Grasping with a step force

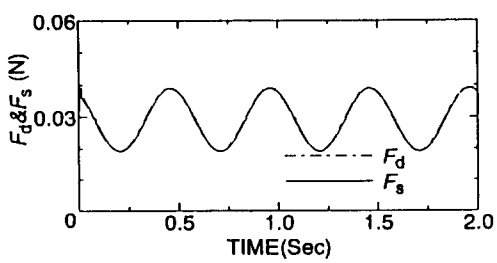

(b) Graping with a time-varying force

Fig. 25. Force response when the finger is controlled so that it holds a statonary object. (a) Grasping with a step force; (b) Graping with a time-varying force.

Figure 25 shows the experimental results when the artificial finger was commanded to hold a stationary object with a prescribed, minute, constant or time-varying force. Figure 25(a) is the results when the finger was driven so that the tip produces a step-command force of amplitude 0.03N.

In the figures, the dashed line shows the commanded constant force 0.03N while the solid line the measurement of the tip force. The one-dotted chained line is the input control voltage to the piezoelectric actuators It is noted that the tip force converges to the commanded value promptly after 0.1 seconds. Figure 25(b) shows the results when the fingertip was driven so that it produces a sinusoidal force of amplitude 0.01N and a mean value of 0.03N. It is found that the fingertip realizes the commanded force variation neatly.

Figure 26 shows the experimental results when the artificial finger was demanded to hold a time-fluctuating object with a constant commanded force.

The fluctuation of the object is a sinusoid and such that it causes a reaction of 0.01N to the finger if the finger is not driven and at the mercy of the object fluctuation.

In the figure, the one dotted chained line shows the commanded constant force 0.03N while the solid line the sensor's measurement of actual tip force.

It is seen that the grasping force is kept constant satisfactorily even if the object is moving.

The results given above show that piezoelectric cells work well as actuators in the vibration control, the precise positioning and the minute force control of the miniature flexible robotic finger.

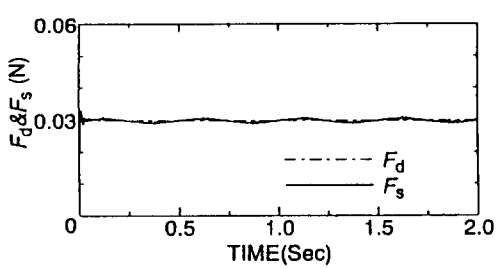

Fig. 26. Force response when the finger is commanded to hold a fluctuating object with a constant force.

Ⅵ. Conclusions

In general, three characteristics are demanded on the modern electro-mechanical machinery. First, they have to be simple and compact and they have to bear high-speed operations. Further, they have to finish sophisticated, high-precision tasks.

To satisfy the first two requirements the total mass of the system should be reduced, which means that the structural stiffness is also decreased and the system is easily excited by the internal as well as external disturbances.

As a result, it is sometimes observed that the high-precision tasks are not accomplished satisfactorily. Thus, the control of the vibration appeared on the high-speed lightweight system is a vital problem to be overcome for the modern machatronic machinery. In the classical passive control of vibration, the total system vibration was first damped out, then the next step of task was started. This was true for the heavy rigid industrial robots. When the active control theory is introduced, it is not necessary to put down the total system vibration. For example, the end effector of the flexible lightweight manipulator is positioned without damping off the total system vibration. Contrary to the rigid arm control, the rest of the manipulator are driven positively by the actuators so thatthe tip stays at its commanded position. Further, the manipulator can do tasks such as keeping a constant distance to the fluctuating target if the end effector is moved actively synchronized with the object.[37]

Introduction of the active control shortens one step of task, and it contributes to the improvement of system productivity.

The active control, however, is quite different from the scheme of classical passive control. It depends on the efficiency of the controller consisting of the sensors, actuators, data processors and computers, which means that the mechanical systems are how much more dependent on the electronic engineering. The fusion of the mechanical engineering with the electronics will contrionte to the development technical innovation in the future.

Acknowledgement

The authors wish to express their sincere thanks to The Korean Institute of Telematics and Electronics for providing the opportunity to summarize this article.

References

[1] Fosdick, F. and Villaggio, P., " Influence of the bending stiffness on the shape of a belt in steady motion", Transactions of the American Society of Mechanical Engine-ers, *Trans. ASME, Journal of Applied Mechanics*, Vol.53, pp.226-270, 1986.

[2] Chilas, T.H.C and Cowburn, A., " Power transmission losses in V-belt drives. Part 2: effect of small pulley sadii", *IMechE, Vol.201(A1)*, pp.41-53, 1987.

[3] Kim, H. and Marshek, K.M., "Belt forces with grinding", Transactions of the American Society of Mechanical Engineers, *Trans.~ASME, Journal of Engineering for industry*, Vol.110, pp.201-211, 1988.

[4] Wang, K.M., " On the stability of chain drive systems under periodic sprocket osciallations", Transactions of the American Society of Mechanical Engineers, *Trans.~ASME, Journal of*

vibration and Acoustics, Vol.114, pp.119-126, 1992.

[5] Oshinoya, Y. and Shimogo, T., " Electromagnetic deviation control of a travelling steel belt", *JSME International Journal*, Vol.35, No.1, pp.109-115, 1992.

[6] Wang, K.W., Liu, S.P., Hayek S.I. and Chen, F.H.K., "On the impact intensity of vibrating axially moving roller chains", Transaction of the American Society of Mechanical Engineers, *Trans. ~ASME. Journal of Vibration and Acoustics*), Vol.114, pp.397-403, 1992.

[7] Hwang, S.-J. and Perkings, N.C., " Supercritical stability of an axially moving beam. Part : Vibration and stability analysis", *Journal of Sound and Vibration*, Vol.154, No.3, pp.379-409, 1992.

[8] Tadikonda, S.S.K. and Baruh, H., " Dynamics and control of a translating frexible beam with a prismatic joint", Transactions of the American Society of Mechanical Engineers, *Trans. ~ ASME. Journal of Dynamic Systems. Measurement. and Control*, Vol.114, pp.422-427, 1992.

[9] Wickert, J.A., " Analysis of self-excited longitudinal vibration of a moving tape", *Journal of Sound and Vibration*, Vol.160, No.3, pp.455-463, 1993.

[10] Tan, C.A., Yang, B. and Mote, JR.C.D., "Dynamic response of an axially moving beam coupled to hydrodynamic bearings", Transactions of the American Society of Mechanical Engineers, *Trans. ASME. Journal of Vibration and Acoustics*, Vol.115, pp.9-15, 1993.

[11] Jiang, Z.W., Chonan, S. and Abe, H., "Effect of the stiffness of pulley mounting system on the stability of axially moving bandeaws",. *Proceedings of International Conference on Mechanical Dynamics, Shenyang, China*, pp.338-343, 1987.

[12] Chonan, S., "Steady state response of an axially moving strip subjected to astationary lateral load", *Journal of Sound and Vibration*, Vol.107(1), 155-165, 1986.

[13] Benson, R.C. and Bogy, D.B., "Deflection of a very Flexible Spinning Disk Due to a Stationary Transverse Load", *Trans. ~ASME. Journal of Applied Mechanics*, Vol.45, pp.636-642, 1978.

[14] Carlin, J.F., F.C., Bridwell, H.C., and Dubois, R.P., "Effects of Tension-ing on Buckling and vibration of Circular Saw Blades", *Trans. ASME. Journal of Engineering for Industry*, Vol.97, pp.37-48, 1975.

[15] Chonan, S., and Sato, S., "Vibration and Stability of Rotating Free-Clamped Slicing Blades", *Journal of Sound and Vibration*, Vol.127, pp.245-252, 1988.

[16] Chonan, S., and Hayase, T., " Stress Analysis of a Spinning Annular Disk to a Stationary Distributed, In-Plane Edge Load", *Trans. ASME, Journal of Vibration, Acoustics, Stress, and Reliability in Design*, Vol.109, pp.277-282, 1987.

[17] Ferguson, N.S., and White, R.G., "The Free Vibration Characteristics of a Clamped-Free Disk Under the Action of a Static In-Plane Load and Constraint on the Outer Periphery", *Journal of Sound and Vibration*, Vol.121, pp.497-509, 1988.

[18] Forman, S.E., and Rhines, W.J., " Vibration Characteristics of Crystal Slicing ID Saw Blades", Journal of the Electrochemical Society, Vol.119, pp.686-690, 1972.

[19] Leung, R.C.N., and Pinnington, R.J., "Vibration of a Rotating Disk Subjected to an In-Plane Force at its Rim, or at

its Center", *Journal of Sound and Vibration*, Vol.114, pp.281-295, 1987.

[20] Hutton, S.G., Chonan, S. and Lehmann, B.F., "Dynamic Response of a Guided Circular Saw", *Journal of Sound and Vibration*, Vol.112(3), pp.527—539, 1987.

[21] Iwan, W.D. and Moeller, T.L., "The Stability of a Spinning Elastic Disk With a Transverse Load System", *Trans. ASME, Journal of Applied Mechanics*, Vol.43, pp.485—490, 1976.

[22] Jiang, Z.W., Chonan, S., "On the Natural Vibration and Method of Analysis of a Rotating Floppy Disk with a R/W Head System", *Transactions of the Japan Society of Mechanical Engineers*, Series C, Vol.54, No.507, pp.2669—2674, 1988.

[23] Ono, K. and Maeno, T., "A Study on the Mechanical Interface Between Head and Media in a Flexible Disk Drive", *Transactions of the Japan Society of Mechanical Engineers*, Series C, Vol.52, No.484, pp.3100—3107, 1986.

[24] Mote, C.~D. Jr., "Moving-Load Stability of a Circular Plate on a Floating Central Collar", *Journal of Acoustical Society of America*, Vol.61(2), pp.439—447, 1977.

[25] Radcliffe, C.J., and Mote, Jr.C.D., "Stability of Stationary and Rotating Disks Under Edge Load", *International Journal of Mechanical Sciences*, Vol.19, pp.567-574, 1977.

[26] Jiang, Z.W., Chonan, S. and Abé, H., "Dynamic Response of a Read/Write Head Floppy Disk System Subjected to Axial Excitation", *Trans. ASME, Journal of Vibration and Acoustics*, Vol.112, No.1, pp.53-58, 1990.

[27] Chonan, S., Mikami, T. and Ishikawa, H., "The Vibrations and Critical Speeds of Rotating Sawblades", *Transactions of the Japan Society of Mechanical Engineers*, Series C, Vol.55, pp.1366-1371, 1986.

[28] Adams, G.G., "Critical Speeds for a flexible spinning Disk", *International Journal of Mechanical Science*, Vol.29, No.8, pp.525-531, 1987.

[29] Chonan, S., Jiang, Z.W. and Shyu, Y.J., " Stability Analysis of a 2' ' Floppy Disk Drive System and the Optimum Design of the Disk Stabilizer", *Trans. ASME, Journal of Vibration and Acoustics*, Vol.114, pp.283-286, 1992.

[30] Jiang, Z.W., Takashima, K. and Chonan, S., "Shock-Proof Design of Head Disk Assembly Subjected to Impulsive Excitation", *Transactions of the Japan Society of Mechanical Engineers*, Series C, Vol.58, pp.3681-3688, 1992.

[31] Chonan, S., Jiang, Z.W. and Yuki, Y., "Vibration and Deflection of a Silicon-Wafer Slicer Cutting the Crystal Ingot", *Trans. ASME, Journal of Vibration and Acoustics*, Vol.115, No.4, pp.529-534, 1993.

[32] Chonan,S., Jiang, Z.W. and Yuki, Y., "Stress Analysis of a Silicon-Wafer Slicer Cutting the Crystal Ingot", *Trans. ASME, Journal of Mechanical Design*, Vol.115, No.4, pp.711-717, 1993.

[33] Cannon, JR.R.H. and Schmitz, E., "Initial experiments on the end-point control of a flexible one-linkrobot", *International Journal of Robotics Research*, Vol.3, No.3, pp.62-75, 1984.

[34] Yuan, B.-S., Book, W.J. and Huggins, J.A., " Dynamics of flexible manipulator arms: Alternative derivation, verification, and characteristics for control",

Transaction of the American Society of Mechanical, *Trans. ASME. Journal of Dynamic Systems. Measurement. and Control*, Vol.115. pp.394-404. 1993.

[35] Eisler, G.R., Robinett, R.D., Segalman, A.J. and Feddema, J.D., "Approximate optimal trajectories for flexible-link manipulator slewing using recursive quadratic programming. Transaction of the American Society of Mechanical, *Trans. ASME. Journal of Dynamic Systems, Measurement. and Control*, Vol.115. pp.405-410. 1993.

[36] Chonan, S. and Umeno, A., Closed-loop end-point control of a two-link flexible arm with a tip mass. *Journal of Sound and Vibration*, Vol.133, pp.483-495. 1989.

[37] Chonan S. and Aoshima, A., End-point control of a flexible arm keeping a constantdistance to fluctuating target ,*Journal of Sound and Vibration*. Vol.142. pp.87-100. 1990.

[38] Chonan, S. and Yamazaki, Y., Out-of-plane position control of a two-link flexiblearm by tip sensing and base torquing", *Journal of Sound and Vibration*. Vol.157. pp.317-330. 1992.

[39] Tahara, M. and Chonan, S., Closed-loop displacement control of a one-link flexible arm witha tip mass. *JSME International Journal. Series* Ⅲ. Vol.31. No.2. pp.409-415. 1988.

[40] Chonan S. and Aoshima, S., 3-Dimensional vibration analysis of multi-link flexible robot arms Transactions of the Japan Society of Mechanical Engineers, Series C. Vol.54. No.502. pp.1170-1175.1988

[41] Chonan, S., Jiang, Z.W. and Taka-hashi, K.,Positioning of a two-link flexible arm using the simple decen-tralized sensing and torquing. *'91 KACC 1*. pp.1441-1446. 1991.

[42] Okada. T., Object-Handling System for Manual Industry", *IEEE Trans. System, Man*, and Cybernetics. SMC-9(2). pp.79-89. 1979.

[43] Salisbury. J.K. and Craig. J.J., Articulated Hands: Force Control and Kinematic Issues. *The International Journal of Robotics Reseach*. Vol.1. No.1. pp.4-17. 1982.

[44] Dario. P. and Buttazzo. G., An Anthropomorphic Robot Finger for Investigating Artificial Tactile Perception", *The International Journal of Robotics Reseach*. Vol.6. No.3., pp.25-48. Fall 1987.

[45] Parker. J.K. and Paul. F.W., Controlling Impact Forces in Pneumatic Robot Hand Design. *Trans.ASME. Journal of Dynamic System. Measurement. and Control*. Vol.109. pp.328-334. 1987.

[46] Whitney. D.E., Force Feedback Control of Manipulator Fine Motions. *Journal of Dynamic System. Measurement. and Control*. Vol.99. pp.91-97. 1977.

[47] Raibert. M.H. and Craig. J.J., Hybrid position/Force Control of Manipulators. *Trans.ASME. Journal of Dynamic System. Measurement. and Control*. Vol.103. pp.126-133. 1981.

[48] Sersji. H., Adaptive Force and Position Control of Manipulators", *Journal of Robotics Systems*. Vol.4. No.4. pp.551-578. 1987.

[49] Ikuta. K., Beard. D.C., Ho. S., and Moiin. H., Direct Stiffness and Force Control of a Shape Memory Alloy-Actuators and Application to Miniature Gripper", *ASME Winter Annual Meeting. San Francisco. U.S.A*. DSC-11. pp.241-246.1989.

[50] Bailey. T. and Hubbard. J.E., Dis-

tributed Piezoelectric-Polymer Active Vibration Control of a Cantilever Beam, *Journal of Guidance and Control*, Vol.8, No.5, pp.605-611, 1985.

[51] Baz, A. and Poh, S., Performance of an Active Control System With Piezoelectric Actuators," *Journal of Sound and Vibration*, Vol.126, No.2, pp.327-343, 1988.

[52] Toda, M., Elastic Properties of Piezoelectric PVF2, *Journal of Applied Physics*, Vol.51, No.9, pp.4673-4677, 1980.

[53] Jiang, Z.W., Chonan, S. and Tan,i J., Position Control of a Flexible Arm Using Piezoelectric Bimorph Cells, *Trans. ASME, Journal of Dynamic System, Measurement, and Control*, Vol.113, No.2, pp.327-329, 1991.

[54] Jiang, Z.W. and Chonan, S., End-Point Force Control of a Miniature Flexible Maniputator Driven by Piezoelectric Cells," *Transactions of the Japan Society of Mechanical Engineers*, Series C, Vol.58, No.548, pp.1120-1127, 1992.

[55] Chonan, S., Jiang, Z.W. and Sakuma, S., Control of a Miniature Gripper Driven by PiezoelectricBimorph Cells," *Transactions of the Japan Society of Mechanical Engineers*,Series C, Vol.59, pp.150-157, 1993.

[56] Jiang, Z.W., Chonan, S. and Tani, J., "Tracking Control of a Miniature Flexible Arm Using Piezoelectric Bimorph Cells", *The International Journal of Robotics Research*, Vol.11, No.3, pp.260-267, 1992.

[57] Jiang, Z.W., Chonan, S., Koseki, M. and Chung, T.J., "Force holding Control of a Finger Using Piezoelectric Actuators", *'93 KACC*, pp.202-207, 1993.

筆者紹介

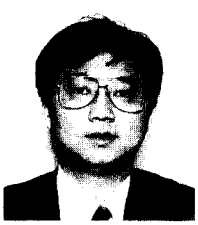

江 鐘 偉(JIANG, Zhong-wei)
September 21, 1958.
Affiliation:
Associate Professor, Department of Aeronautics and Space Engineering, Tohoku University, Sendai, Japan.

Zhong-wei Jiang is an associate professor of Aeronautics and Space Engineering Department at Tohoku University, Sendai, Japan. He received his BS degree in 1982 in Mechanical Engineering from Northeastern University, China and MS and Ph.D in Mechanical Engineering from Tohoku University, Japan in 1987 and 1990.

His current research interests include dynamics and control of robotic arms/fingers, magnetic head/disk assemblies, circular and band saws, piezoelectric sensors/actuators, SMA actuators, soft sensors and electronic and mechanical equipments.

筆 者 紹 介

長 南 征 二 (CHONAN, Seiji)
November 12, 1942

Affiliation:
Professor, Department of Aeronautics and Space Engineering, Tohoku Uiversity, Sendai, Japan.

Seiji Chonan is a professor of Aeronautics and Space Engineering Department at Tohoku University, Sendai, Japan. He received his BS degree in 1966, and MS and Ph.D in Mechanical Engineering from Tohoku University in 1968 and 1971. He was invited as a visiting professor at University of British Columbia, Canada in 1983, at Chonbuk Uiversity, Korea in 1987 and 1993, and as an exchange professor at Northeastern University, China in 1988. He has authored or coauthored a technical book, more than 90 refereed international and domestic journal papers, 22 international conference papers, 12 technical reports, and 4 international patents. He organized the first Japan-Korea Joint Seminar on Advanced Mechatronics in Sendai, Japan in 1992. He is the chairman of the technical section on hypertechnology in dynamics, control and acoustics, JSME. His current research interests include dynamics and control of robotic arms/fingers, head/tape assemblies, silicon wafer slicers, piezoelectric sensors/actuators,

SMA actuators, tribo-sensors, soundproof walls and shells, and electronic and mechanical equipments.